Mapping Flow and Dispersion in a Packed Column by MRI

Jaekeun Park and Stephen J. Gibbs
Center for Interdisciplinary Magnetic Resonance, National High Magnetic Field Laboratory, Florida State University, 1800 E. Paul Drive, Tallahassee FL 32310

and

Dept. of Chemical Engineering, FAMU-FSU College of Engineering, Tallahassee FL 32310

Fluid flow and dispersion in porous media are important in many contexts including hydrology, oil recovery, chemical reaction engineering, chemical separations, composite materials processing, biology, and medicine. Of particular importance in many separations operations such as adsorption or chromatography is the uniformity of the fluid-flow field and the minimization of axial dispersion, which are crucial for maximizing the efficiency of the separation process. The porous medium in these cases is typically a packed or consolidated bed of porous particles. Because of the extreme sensitivity of the local permeability of the packed bed to the local packing density (or void fraction), as expressed in the Blake–Kozeny equation, it is imperative that columns be packed as uniformly as possible in order to achieve uniform fluid velocities throughout the column. It is also important that column headers distribute flow uniformly and that uniform temperature be maintained over the column cross section.

Several strategies have been developed for introducing particles to the column and consolidating the bed. These include dry packing, slurry packing, column vibration, axial compression, and radial compression, and have recently been reviewed by Guiochon et al. (1997). There is an increasingly large body of evidence that suggests that most of these techniques yield a packing density that is radially nonuniform; the results of several measurements indicate that, for axially compressed columns, the fluid velocity near the wall of the column can be substantially less than in the column center (Yun and Guiochon, 1997; Guiochon et al., 1997). Further, macroscopic measures of column efficiency via a height equivalent of a theoretical plate (HETP or H) indicate a dramatically larger plate height near the column wall than near the column center.

We report here spatially resolved measurements of fluid velocity and apparent dispersion coefficient in a packed column of impermeable polystyrene beads by magnetic-resonance-imaging velocimetry (MRIV). The measurements show that in our column, there is a gradual decrease in fluid velocity from the column center to a distance of about eight particle diameters from the wall, followed by a dramatic decrease to a minimum velocity at about three particle diameters from the wall. Our measurements may show larger radial variation in the axial velocity than other measurement techniques on the same column because the MRIV technique employed measured fluid displacements of only tens of particle diameters; hence, transverse dispersion does not significantly flatten the observed velocity profile in these short-time measurements.

Magnetic Resonance Velocimetry Methods

Several reports of magnetic-resonance applications to studying transport in packed columns have appeared recently (Chen et al., 1993; Rajanayagam et al., 1995; Hoffman et al., 1996; Kutsovksy et al., 1996; Lightfoot et al., 1997; Sederman et al., 1997; Feinauer et al., 1997; Mitchell et al., 1997; Van As and van Dusschoten, 1997). Many of these are based on the pulsed-field-gradient (or PFG) technique in which it is possible to measure the spectrum of molecular displacements (or propagator) over a time interval Δ (Callaghan, 1991; Baumeister et al., 1995; van Dusschoten et al., 1997; Tallarek et al., 1998). The consensus of several recent publications is that for flow in several types of porous media including packed beds of impermeable spheres and natural porous rock, the shape of the spectrum of molecular displacements depends strongly upon the quantity $\Delta v/d_p$, where Δ is the time allowed for the displacements to occur, v is the interstitial fluid velocity, and d_p is the average particle size of the porous medium (Lebon et al., 1996, 1997; Packer and Tessier, 1996; Tessier and Packer, 1998). For small $\Delta v/d_p$ the propagator is very asymmetric; it reflects the instantaneous velocity distribution in the channels and pores of the medium. For large $\Delta v/d_p$, the propagator becomes nearly Gaussian. For inter-

Correspondence concerning this article should be addressed to S. J. Gibbs.

mediate $\Delta v/d_p$, behavior can be very complex; for packed beds of uniformly sized, impermeable spheres, multimodal propagators have been observed with the various modes corresponding to the preferred displacements of an integer number of interstices between particles (Seymour and Callaghan, 1996; Amin et al., 1997).

The NMR pulse sequences employed in our work are shown in Figure 1a. The first part of the sequence is an alternating-direction, pulsed-gradient, stimulated-echo sequence used for motion encoding (Cotts et al., 1989). Magnetization encoded in this fashion is then stored longitudinally for later readout by either (1) a slice-selective gradient echo used for our measurements of displacement spectra averaged over the entire column cross section, or (2) a slice-selective *spin-warp spin-echo* sequence used to obtain spatially resolved measures of fluid percolation velocity (Callaghan, 1991). The phase cycling used for both the imaging and bulk displacement spectra studies is a 32-element cycle designed to eliminate unwanted echoes and signal resulting from longitudinal relaxation during the storage periods.

In the short gradient-pulse approximation, negligible motion occurs during the gradient-pulse intervals 2τ, and the stimulated echo signal can be represented by (Callaghan, 1991)

$$S(q,\Delta) = \int \rho(r) \int P_s(r|r',\Delta) \exp\left[i2\pi q\cdot(r'-r)\right] dr'|dr, \quad (1)$$

where $q = (2\pi)^{-1}\gamma\delta g$ [cycles/m] and can be thought of as the wave vector for motion encoding; r is position; $\rho(r)$ is the nuclear spin density; and $P_s(r|r',\Delta)$ is the probability of a nuclear spin initially at location **r** moving to location r' in the time interval Δ; and g is the pulsed magnetic-field gradient. Fourier transformation of $S(q,\Delta)$ with respect to **q** then permits the determination of the spatially averaged propagator or displacement spectrum given by $\overline{P_s}(\mathbf{R},\Delta) = \int \rho(r) P_s(r|r+R,\Delta)dr$, where $R = r' - r$. Note that in the preceding treatment we have neglected nuclear relaxation, inflow/outflow, and chemical shift and coupling effects.

Measurements described herein were performed with a Bruker Avance DMX spectrometer operating at 600 MHz for protons and coupled with a 14-tesla, 89-mm-bore Bruker/Magnex magnet. This system is equipped with an actively shielded gradient set capable of switching 0.96 T/m in 110 μs at 40 A. A 25-mm-ID "bird cage"-type resonator was used for the radio-frequency coil. The active length of the resonator is approximately 40 mm.

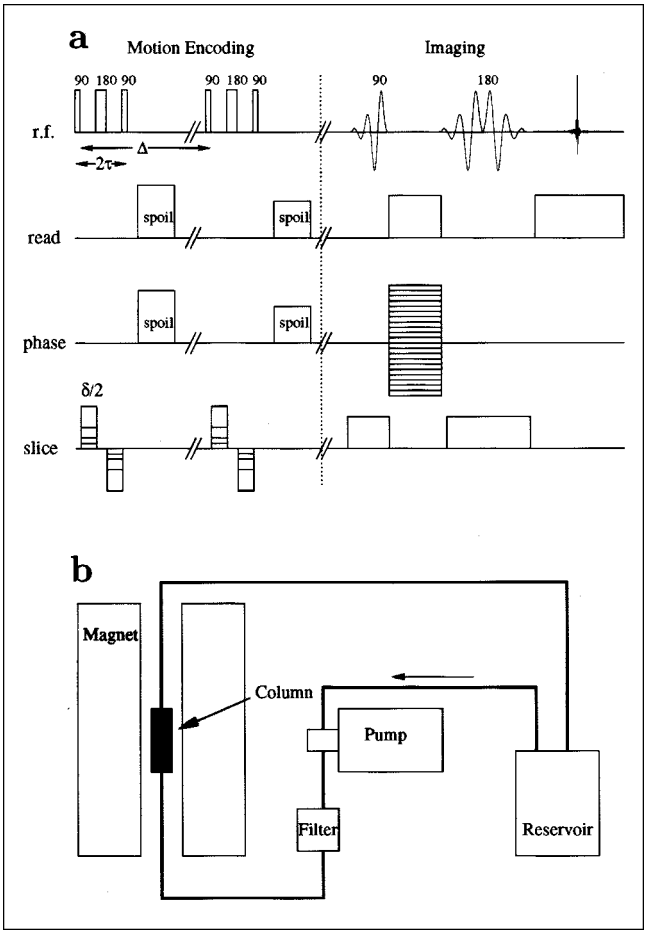

Figure 1. (a) Timing diagram for the NMR pulse sequence; (b) flow system and NMR magnet.

For the bulk displacement spectra, the imaging section of the pulse sequence was replaced by a slice-selective gradient echo.

Column Packing

An 11.7-mm-ID column (BioSepra, Marlborough, MA) was slurry packed with 99-μm-diameter polystyrene beads (Bangs Laboratories, Fishers, IN). The column was packed by gravity flow of an aqueous suspension of beads containing 0.005% of the surfactant Triton X-100 in order to thoroughly wet the bead surfaces and a small amount of bacteriostat (Sigma Clean water bath treatment). The top distributor was then replaced and the bed slightly axially compressed in order to remove air spaces near the top of the column. The column was then placed in the radio-frequency probe and inserted into the bore of the NMR magnet, as shown in Figure 1b. Flow at 0.12 mL/s was provided by a piston pump (SciLog, Inc., Madison, WI).

Bulk Displacement Spectra

Bulk displacement spectra for a 5-mm-thick slice of the column were obtained for a range of evolution times and are shown in Figure 2. For short evolution times the spectra are asymmetric, but for long times the spectra become nearly Gaussian. For the three long-time spectra in Figure 2b, the data are well fit by the displayed Gaussian curves with dispersion coefficients of 0.13, 0.16 and 0.17 mm^2 for 207, 507 and 1,007 ms, respectively. These values correspond to reduced plate heights $h = H/d_p$ of 0.92, 1.1, and 1.1. The 1007-ms spectrum shows a tailing deviation from Gaussian behavior that may be due to a spatially inhomogeneous flow field over the column cross section. Pore scale velocity inhomogeneity causes the short-time spectral broadening and asymmetry; these inhomogeneities should be averaged to produce a Gaussian spectrum on a time scale of d_p/v. Larger, column-scale inhomogeneities will take much longer to average.

The displacement spectra shown in Figure 2 were obtained by Fourier transforming 128 pulsed-gradient echoes, ac-

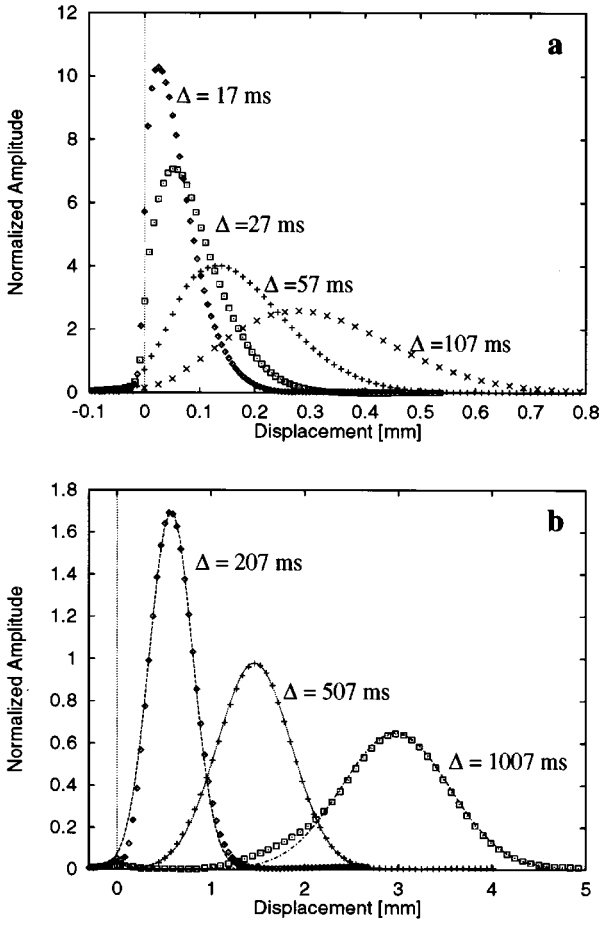

Figure 2. Displacement spectra (or propagators) for the flowing fluid in a packed bed of impermeable polystyrene spheres for a range of evolution times Δ.

Note that the spectra are nearly Gaussian for long Δ in (b). Points are experimental data for a 5-mm slice and lines are Gaussian curves.

quired with positive- and negative-gradient amplitudes along the axis of the column for full echo acquisition, with respect to the amplitude of the pulsed gradient (Callaghan, 1991). Acquiring data for both positive- and negative-gradient amplitudes permits calculation of magnitude spectra without contamination of the spectra by *dispersion-mode* signal.

The spectra do not exhibit the multimodal behavior at intermediate evolution times reported by Amin et al. (1997). We have, however, observed multimodal behavior for other columns packed with impermeable beads. The lack of multimodal displacement spectra for intermediate times in the column considered here may be a result of the spatially inhomogeneous velocity field as demonstrated below.

Velocity and Dispersion Maps

These data demonstrate the approach to Gaussian behavior for long evolution times Δ and hence suggest the approach used for mapping fluid velocity and dispersion over the column cross section. If the assumption of a Gaussian displacement spectrum is valid for each pixel, then it is not necessary to acquire data corresponding to a large number of pulsed gradient or **q** amplitudes. Rather, a limited number of images can be acquired for a small number of pulsed-gradient values. By fitting a Gaussian damped sinusoid.

$$S = S_0 \exp\left[-(2\pi q)^2 \mathfrak{D}\Delta + i((2\pi q)v\Delta + \phi)\right] \qquad (2)$$

to the data from each pixel with S_0, v, $\mathfrak{D}$, and ϕ as free parameters, where v is the fluid velocity, Δ is the evolution time, $\mathfrak{D}$ is the apparent diffusion or dispersion coefficient, and ϕ is an arbitrary phase angle, it is possible to estimate reliably these values at each pixel. Precision in estimating the adjustable parameters is typically on the order of 1 to 5% (Gibbs et al., 1996).

Figure 3 shows example data from single pixels as a function of the applied magnetic-field gradient and the velocity map obtained by fitting Eq. 2 to data collected for $\Delta = 1.01$ s, $\delta = 2$ ms. Fourteen images were acquired with the same 32 transient phase cycle used for the bulk-displacement spectra for values of g_z ranging from 1.0×10^{-4} mT/m to 2.0×10^{-2} mT/m. The image matrices are 128×128 pixels for a 1.4-cm field of view. The data in Figures 3a and 3b are from pixels near the center and near the wall of the column, respectively, and the smooth curves are least-squares fits of Eq. 2 to the data. It is clear that the fluid velocity near the wall is significantly less than that near the column center. The velocity map in Figure 3c appears roughly symmetric about the center of the column and suggests further analysis of the data by plotting velocity vs. radial position. The procedure for going from the two-dimensional Cartesian map to a radial plot is simple in principle, but several important details are discussed by Gibbs et al. (1996).

The radial plot of velocity in Figure 4a shows a striking and systematic decrease in the apparent velocity from the center of the column to a distance approximately eight particle diameters from the wall. Over this distance, the fluid velocity decreases from about 0.33 cm/s at the column center to approximately 0.26 cm/s. The velocity then arbruptly decreases to 0.20 cm/s at a distance of about three particle diameter from the column wall. At radial positions closer than three particle diameters from the wall, the apparent fluid velocities are more highly scattered than those nearer the center of the column, but on average increase as the wall is approached. These three general features of the radial-velocity distribution have been reproduced for three other columns packed in the same way with the same materials, but much more uniform velocity profiles have been observed for porous, compressible packing materials.

Guiochon et al. (1997) have recently reviewed reports of inhomogeneity in the velocity field in chromatographic columns. Our results are consistent with the trends observed for other slurry packed, axially compressed columns, but show a much larger degree of inhomogeneity. The larger velocity inhomogeneity in our case may be due to an actual greater variation in packing density, but also due to less time being allowed for averaging of the velocity field by radial dispersion in the short-time PFG NMR measurements as compared with macroscopic impulse-response measurements.

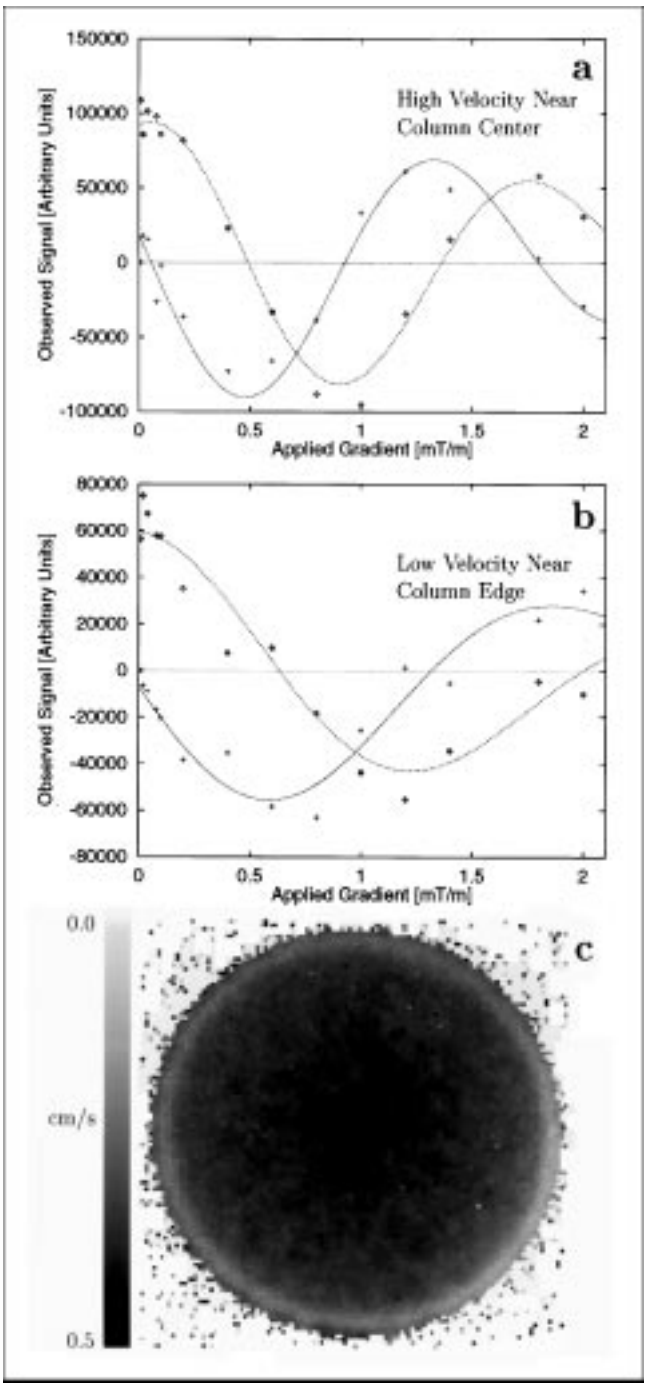

Figure 3. (a,b) NMR signal from single pixels as a function of pulsed gradient amplitude for $\Delta \approx 1$ s; (c) resulting 128×128 pixel velocity map for a 6-mm slice through the column.

Shown are the real and imaginary parts of the experimental data (points) and the best fit of a Gaussian damped sinusoid (Eq. 2) (lines). The data in (a) are from a pixel near the center of the column and the data in (b) are from the edge of the column. Black represents 0.5 cm/s and white 0.0 cm/s.

Since the NMR technique employed measures the interstitial fluid velocity rather than the superficial velocity, measuring the total flow rate Q allows calculation of the column void fraction ϵ_b provided that the column cross-sectional area is known, according to $Q = Av_0 = A\epsilon_b\langle v\rangle$, where A is the column cross section and $\langle v\rangle$ is the cross-sectionally averaged interstitial fluid velocity. The cross-sectionally averaged velocity determined from the NMR data in Figure 4a is 0.28 cm/s; in combination with the overall flow rate of 0.12 mL/s, measured by timed mass collection, this intersitial velocity in-

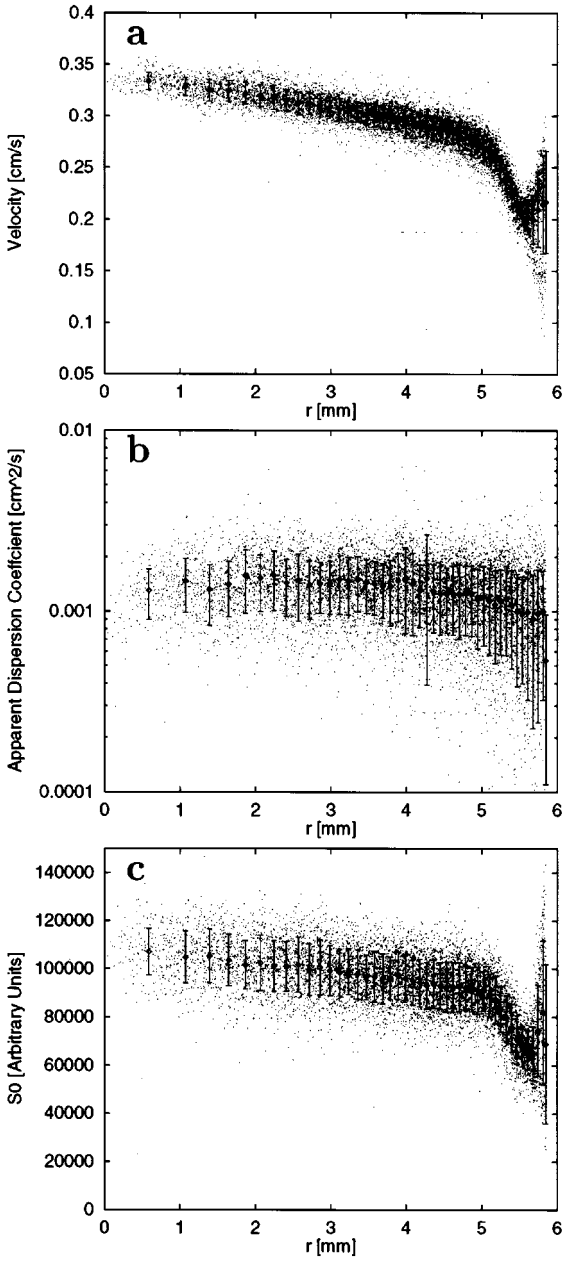

Figure 4. Radial profiles of apparent (a) fluid velocity, (b) dipersion coefficient, and (c) nuclear magnetization measured by MRI for water flow in the 11.7-mm-diameter column packed with 99-μm-diameter polystyrene beads.

Dots represent measurements from a single pixel. Points represent the average of 200 pixel measurements in a given radial bin; error bars represent the standard deviations of those 200 measurements.

dicates an average column void fraction of 0.4. This calculation is, however, very sensitive to the exact value of the column internal diameter used; here we have used a diameter of 11.7 mm as determined from several caliper measurements.

The radial plot of apparent axial dispersion coefficient in Figure 4b shows a gradual decrease of the apparent axial dispersion coefficient with increasing radial position. This decrease is nearly proportional to the observed velocity decrease, but the dispersion data are noisier. This observation is in contrast with the majority of those reviewed by Guiochon et al. (1997) in which the apparent plate height or dispersion coefficient was found to increase dramatically near the column wall. Again, this difference between the macroscopic tracer measurements and the short-time PFG NMR measurements is consistent with radial dispersion acting to flatten the observed velocity profile and increase the observed dispersion coefficient in regions of velocity-field inhomogeneity.

The results of many observations in packed beds suggest that the long-time axial dispersion coefficient can be correlated by $\mathcal{E}/\mathcal{D} \approx N_{Re}N_{Sc}$ for $N_{Re}N_{Sc} \gg 1$, where $N_{Re}N_{Sc} = d_p v \epsilon_b/\mathcal{D}$. For our conditions, $N_{Re}N_{Sc} \approx 49$ and the observed pixel average $\mathcal{E} = 1.3\times10^{-3}$ cm^2·s, making $\mathcal{E}/\mathcal{D} = 56$. This value corresponds to a reduced plate height $h = H/d_p$ of approximately 0.9, and is less than the bulk values observed at 507 and 1,007 ms, and is thus consistent with significant dispersion being caused by macroscopic flow field inhomogeneity. It is interesting to study the experimental data of Magnico and Martin (1990) on carefully packed beds of impermeable glass beads; for the same reduced velocity as in our measurements, they observed a reduced plate height of approximately 2.

Figure 4c shows the dependence of NMR signal intensity S_0 with radial position in the column; this dependence mimics that of the fluid velocity. Variations in S_0 must be due either to variations in the local water density in the column or to variations in the effective nuclear relaxation times, or to both. The first of these would be directly related to variations in the local packing density; however, it seems unlikely that the column void fraction could change enough to account for the nearly factor of 2 change in S_0 from the wall region to the center of the column. The local nuclear relaxation times in the column will depend on the local surface-to-volume ratio, and hence both on the local packing density and the local particle size distribution. We have obtained similar S_0 maps for stationary fluid and different packed columns (using the same packing techniques and the same materials).

At this stage it is impossible to determine whether the observed dependence of v and S_0 upon radial position in the column are due to radial variations in packing density alone, particle-size distribution alone, or some combination of these effects. Careful NMR relaxometry and finer spatial resolution NMR imaging may provide some clues. It will also be important to measure axial variations in packing density and fluid velocity and to determine effects of flow distributor design on the fluid velocity distribution. Further, it will be important to quantitatively account for the smoothing effects of transverse dispersion on the observed radial variation in the axial velocity in order to understand the correspondence between macroscopic column measurements and MRI velocity maps. In combination with traditional impulse-response measurements, NMR imaging methods show tremendous promise for understanding many of the mysteries of column packing techniques and degradation of column performance with time.

Acknowledgments

This work was supported by the FAMU-FSU College of Engineering and the National High Magnetic Field Laboratory. The authors thank Drs. Jonathan Coffman and Bruce Locke for helpful discussions.

Literature Cited

Amin, M. H. G., S. J. Gibbs, R. J. Chorley, K. S. Richards, T. A. Carpenter, and L. D. Hall, ''Study of Flow and Hydrodynamic Dispersion in a Porous Medium Using Pulsed-Field-Gradient Magnetic Resonance,'' *Proc. Roy. Soc. Lond. A*, **453**, 489 (1997).

Baumeister, E., U. Klose, K. Albert, E. Bayer, and G. Guiochon, ''Determination of the Apparent Transverse and Axial Dispersion Coefficients in a Chromatographic Column by Pulsed Field Gradient Nuclear Magnetic Resonance,'' *J. Chromatog. A*, **694**, 321 (1995).

Callaghan, P. T., *Principles of Nuclear Magnetic Resonance Microscopy*, Oxford Univ. Press, New York (1991).

Chen, S., F. Qin, K.-Y. Kim, and A. T. Watson, ''NMR Imaging of Multiphase Flow in Porous Media,'' *AIChE J.*, **39**, 925 (1993).

Cotts, R. M., M. J. R. Hoch, T. Sun, and J. T. Markert, ''Pulsed Field Gradient Stimulated Echo Methods for Improved NMR Diffusion Measurements in Heterogeneous Systems,'' *J. Magn. Reson.*, **83**, 252 (1989).

Feinauer, A., S. A. Altobelli, and E. Fukushima, ''NMR Measurements of Flow Profiles in a Coarse Bed of Packed Spheres,'' *Magn. Reson. Imaging*, **15**, 479 (1997).

Gibbs, S. J., K. L. James, L. D. Hall, D. E. Haycock, W. J. Frith, and S. Ablett, ''Rheometry and Detection of Apparent Wall Slip for Poiseuille of Polymer Solutions and Paticulate Dispersions by Nuclear Magnetic Resonance Velocimetry,'' *J. Rheol.*, **40**, 425 (1996).

Guiochon, G., T. Farkas, H. G. Sajonz, J. H. Koh, M. Sarker, B. J. Stanley, and T. Yun, ''Consolidation of Particle Beds and Packing of Chromatographic Columns,'' *J. Chromatog. A*, **762**, 83 (1997).

Hoffman, F., D. Ronen, and Z. Pearl, ''Evaluation of Flow Characteristics of a Sand Column Using Magnetic Resonance Imaging,'' *J. Contam. Hydrol.*, **22**, 95 (1996).

Kutsovsky, Y. E., V. Alvarado, H. T. Davis, L. E. Scriven, and B. E. Hammer, ''Dispersion of Paramagnetic Tracers in Bead Packs by T_1 Mapping: Experiments and Simulations,'' *Magn. Reson. Imaging*, **14**, 833 (1996).

Lebon, L., L. Oger, J. Leblond, J. P. Hulin, N. S. Martys, and L. M. Schwartz, ''Pulsed Gradient NMR Measurements and Numerical Simulation of Flow Velocity Distribution in Sphere Packings,'' *Phys. Fluids*, **8**, 293 (1996).

Lebon, L., J. Leblond, and J. P. Hulin, ''Experimental Measurement of Dispersion Processes at Short Times Using a Pulsed Field Gradient NMR Technique,'' *Phys. Fluids*, **9**, 481 (1997).

Lightfoot, E. N., J. L. Coffman, F. Lode, Q. S. Yuan, T. W. Perkins, and T. W. Root, ''Refining the Description of Protein Chromatography,'' *J. Chromatog. A*, **760**, 139 (1997).

Magnico, P., and M. Martin, ''Dispersion in the Interstitial Space of Packed Columns,'' *J. Chromatogr.*, **517**, 31 (1990).

Mitchell, N. S., L. Hagel, and E. J. Fernandez, ''In Situ Analysis of Protein Chromatography and Column Efficiency Using Magnetic Resonance Imaging,'' *J. Choromatog. A*, **779**, 73 (1997).

Packer, K. J., and J. J. Tessier, ''The Characterization of Fluid Transport in a Porous Solid by Pulsed Gradient Stimulated Echo NMR,'' *Molec. Phys.*, **87**, 267 (1996).

Rajanayagam, V., S. Yao, and J. M. Pope, ''Quantitative Magnetic Resonance Flow and Diffusion Imaging in Porous Media,'' *Magn. Reson. Imaging*, **13**, 729 (1995).

Sederman, A. J., M. L. Johns, A. S. Bramley, P. Alexander, and L. F.

Gladden, ''Magnetic Resonance Imaging of Liquid Flow and Pore Structure within Packed Beds,'' *Chem. Eng. Sci.*, **52**, 2239 (1997).
Seymour, J. D., and P. T. Callaghan, ''Flow-Diffraction Structural Characterization and Measurement of Hydrodynamic Dispersion in Porous Media by PGSE NMR,'' *J. Magn. Reson. A*, **122**, 90 (1996).
Tallarek, U., E. Bayer, and G. Guiochon, ''Study of Dispersion in Packed Chromatographic Columns by Pulsed Field Gradient Nuclear Magnetic Resonance,'' *J. Amer. Chem. Soc.*, **120**, 1494 (1998).
Tessier, J. J., and K. J. Packer, ''The Characterization of Multiphase Fluid Transport in a Porous Solid by Pulsed Gradient Stimulated Echo Nuclear Magnetic Resonance,'' *Phys. Fluids*, **10**, 75 (1998).
Van As, H., and D. van Dusschoten, ''NMR Methods for Imaging of Transport Processes in Micro-Porous Systems,'' *Geoderma*, **80**, 389 (1997).
van Dusschoten, D., J. van Noort, and H. Van As, ''Displacement Imaging in Porous Media Using the Line Scan NMR Technique,'' *Geoderma*, **80**, 405 (1997).
Yun, T., and G. Guiochon, ''Visualization of the Heterogeneity of Column Beds,'' *J. Chromatog. A*, **760**, 17 (1997).

Manuscript received July 14, 1998, and revision received Dec. 23, 1998.